ELSEVIER

Surface Science 419 (1999) 134–143

surface science

Morphology of ultrathin manganese silicide on Si(111)

Tadaaki Nagao [a,b,*], Satoru Ohuchi [a], Yasuyuki Matsuoka [a], Shuji Hasegawa [a,b]

[a] *Department of Physics, Graduate School of Science, University of Tokyo, 7-3-1 Hongo, Bunkyo-ku, Tokyo 113-0033, Japan*
[b] *Core Research for Evolutional Science and Technology (CREST), Japan Science and Technology Corporation (JST), 4-1-8 Honcho, Kawaguchi, Saitama 332-0012, Japan*

Received 11 May 1998; accepted for publication 7 September 1998

Abstract

Aggregates of Mn atoms adsorbed on Si(111)-(7×7) react with the substrate and form very flat islands terminated with a well ordered ($\sqrt{3}\times\sqrt{3}$) surface ranging up to several hundreds of angstroms. The Si atoms in the DAS (dimer-adatom-stacking fault) structure mostly adjacent to step edges are stripped off to form the flat silicide islands. Island height and diameter of the silicide islands on the (7×7) surface are found to change drastically by changing the annealing time, annealing temperature, and the Mn coverage after room temperature deposition. Mn adsorption and silicide formation of some noble metal precovered Si(111) surfaces were also studied. Different morphologies were observed on each surface [($\sqrt{3}\times\sqrt{3}$)-Ag, ($\sqrt{3}\times\sqrt{3}$)-Au, (6×6)-Au], which indicates the different diffusion lengths and reactivity of the Mn atoms on each surface.

Keywords: Epitaxial growth; Manganese; Morphology; RHEED; Silicon; STM

1. Introduction

The combination of semiconductors and metals is of increasing importance from both technological and fundamental points of view. Recently, epitaxial growth of noble metal silicides or refractory metal silicides have attracted much interest since they are strong candidates for the components of new microelectronic devices. Among them, manganese silicide, for example $MnSi_{1.7}$, was found as semiconducting [1,2] and can be a promising material for silicon-based optoelectronic devices as well as a thermoelectric material for high-temperature applications. However, in contrast to the case of other transition metal silicides (e.g. $FeSi_2$, $CoSi_2$, $CrSi_2$, $NiSi_2$), only a few studies have dealt with the initial stage of epitaxial growth of Mn on silicon surface [3,4].

In this paper, we report the growth of ultra-thin manganese silicide formed epitaxially on Si(111) by RHEED (reflection-high-energy electron diffraction) and STM (scanning tunneling microscopy). Morphology of the quasi two-dimensional silicide islands was found to change dramatically depending on the Mn coverage, the annealing time, and the annealing temperature after room temperature (RT) deposition. A detailed study of controlling the nano-structure of epitaxial silicides might open up the exciting prospect of handling the novel classes of morphology-dependent transport phenomena such as giant magneto resistance, surface conductivity etc. Formation of the manganese silicide on some noble metal precovered

* Corresponding author. Fax: +81 3 5800 3329; e-mail nagao@phys.s.u-tokyo.ac.jp

0039-6028/99/$ – see front matter
PII: S0039-6028(98)00771-7

Si(111) surfaces is also discussed in comparison with the case of the Si(111)-(7×7) surface.

2. Experimental

The experiments were done in an ultrahigh vacuum (UHV) chamber with 4×10^{-11} Torr base pressure which consists of a RHEED chamber for in situ observation of the film structure, and a STM chamber for atomic-image observation of the films after preparation. Commercial p-type high-doped Si wafers with 0.6 mm^{t} oriented to a $\langle111\rangle$ axis with a precision of 0.1° were cleaned in the UHV chamber by repeated cycles of flash heating up to 1500 K. The metals (Mn, Ag and Au) were evaporated from outgassed alumina-coated tungsten baskets with keeping the pressure below 1×10^{-9} Torr during the evaporation. Coverages of deposited noble metals were derived from the duration times which were calibrated to the period needed to complete the $(\sqrt{3}\times\sqrt{3})$ structures. In case of Mn, the coverage was derived from the duration time calibrated to the period for the extinction of the (7×7) superlattice spots in RHEED during RT deposition. This coverage was roughly estimated to be around one monolayer (1 ML) by comparing the total volume of the silicide islands in our STM images with that reported by Evans et al. [4]. It should be carefully noted that the present tentative coverage calibration will include some error since the statistics of the STM data presented in the literature is not high enough. Here, 1 ML means that the number density of adsorbed atoms is equal to that of the Si atoms in the topmost layer of an ideally truncated (111) face. Sample temperature was derived from DC heating current through the sample using calibration plot of the heating current versus sample temperature which was determined by optical pyrometry before the experiment. Precision of the temperature determination including the effect of temperature gradient within the sample is ±30 K. The RHEED pattern was taken at a primary energy of 15 kV and a glancing angle of 2°. This small glancing angle was employed in order to enhance the character of transmission through three-dimensional islands in electron diffraction. Also, extinction of the (7×7) spots during Mn deposition observed at this glancing angle was found to correspond roughly to 1 ML. All the STM pictures (except Fig. 1g) taken here were recorded at positive tip bias between 0.8 and 1.0 V and tunneling current of 0.4–1.0 nA in topographic mode.

3. Results and discussion

3.1. Mn adsorbed on Si(111)-(7×7)

The RHEED and STM results shown in this report were obtained from the surfaces prepared by heating the substrates after Mn deposition at RT. In situ observation of the film growth on heated substrates will be reported elsewhere.

The RHEED patterns and the STM images of Mn/Si(111)-(7×7) heated up to 800 K are shown in Fig. 1. Fig. 1a and e show the pattern and the image of as-deposited Mn film of 1 ML. At the glancing angle of 2° as is shown in Fig. 1a, the (7×7) superlattice spots disappears just at this coverage. However, with larger glancing angles (e.g. 4°) the RHEED pattern shows very weak but sharp (7×7) spots with high background, indicating the presence of the (7×7) interface. Instead of the dimer-adatom-stacking fault (DAS) structure of the (7×7) surface, dull protrusions due to the adsorbed Mn clusters can be seen in Fig. 1e. These irregular Mn clusters have an average size close to that of the (7×7) unit cell. This strongly suggests that the DAS structure of the underlying (7×7) surface is not destroyed severely and thus the diffusion of the impinging Mn atom is restricted within the unit cell of the (7×7) superstructure. As is clear from the STM images of the clean (7×7) surface, change in the electronic state is largest across the dimer rows, which indicates that the potential felt by a Mn atom should also change strongly across them. This potential variation must cause a barrier for Mn hopping between the (7×7) unit cell. This potential barrier will be overcome at elevated temperatures. In fact, a STM image taken after heating at 700 K for 15 s showed that the unreacted Mn clusters grow into one

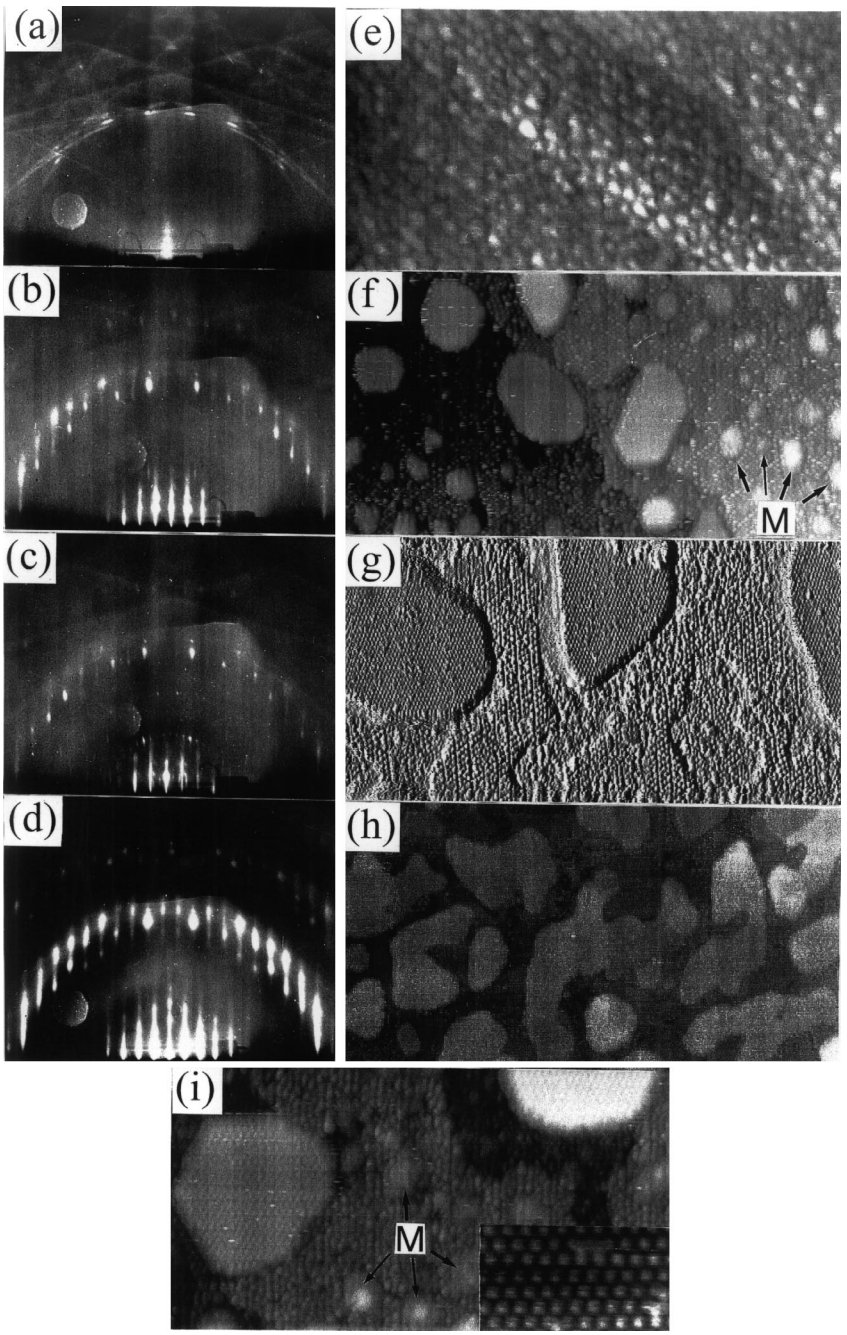

Fig. 1. RHEED patterns (a–d) and STM images (e–i) of Mn deposited on the Si(111)-(7 × 7) surface. (a) and (e) (850 Å × 480 Å) after the deposition of 1 ML of Mn at RT. (b) and (f) (850 Å × 480 Å) after depositing 1 ML of Mn and heated at 800 K for 15 s. (c) and (g) (850 Å × 480 Å) after depositing 1 ML of Mn and heated at 800 K for 900 s and (h) (2000 Å × 1070 Å) after depositing 2 ML of Mn at RT and heating at 800 K for 15 s. (i) A 450 Å × 240 Å STM image of the surface corresponding to (b) and (f). Inset shows a 72 Å × 40 Å image on the $\sqrt{3}$ silicide island. (g) was taken in current imaging mode at 1 V tip bias. Other images were recorded in topographic mode.

another and slightly defective DAS structure of the bare (7×7) surface reappeared.

Fig. 1b and f correspond to the surface heated at 800 K for 15 s. RHEED pattern shows diffuse $(\sqrt{3}\times\sqrt{3})$ streaks as well as very weak (7×7) spots. A STM image of Fig. 1f shows that the (7×7) region has a high density defect, which is consistent with the RHEED observation. The density of small Mn clusters (marked M) is decreased at regions close to steps. At the steps, large tabular islands 4 ± 0.2 Å in height were observed. In Fig. 1i, magnified images taken at a different place of the same sample are shown. The well ordered $(\sqrt{3}\times\sqrt{3})$ structure is clearly recognized on the surface of the tabular islands. Regions close to the tabular islands are severely disordered indicating that the Si atoms in the DAS structure are incorporated into the islands to form silicide (e.g. the depressed region adjacent to the island in the upper right of Fig. 1i). So we call these tabular islands as the $\sqrt{3}$ silicide islands hereafter. On the other hand, atomic structure on the Mn clusters seems rather featureless. The (7×7) structure around the irregular Mn clusters (marked M) is not so much destroyed, which again indicates that they are not reacting severely with the substrate.

Fig. 1c and g correspond to the surface heated at 800 K for 900 s. Irregular Mn clusters like those marked M in Fig. 1f and i are completely absent in Fig. 1g. Instead, area of the $\sqrt{3}$ silicide islands is increased. Around these islands, depressed regions are formed, and their area is roughly equal to those of the $\sqrt{3}$ silicide islands. Depth of these craters is Si-bilayer depth (3 ± 0.2 Å) and the structure at the bottom is disordered. If we assume that the interface between the $\sqrt{3}$ silicide islands and the Si substrate locates at the level of the bottom of the crater, then, the number of the Si atoms incorporated into the $\sqrt{3}$ silicide islands can be roughly estimated to be 1 ML. Since the deposited Mn is about 1 ML here, the ratio between Si and Mn atoms in the $\sqrt{3}$ silicide islands is about 1:1. However, since the calibration of the absolute coverage in the present study is crude further investigation concerning the chemical composition and the atomic structure is required for the precise discussion.

Fig. 1d and h show the RHEED pattern and the STM image of the surface formed after depositing 2 ML of Mn and heated at 800 K for 15 s, respectively. Brighter regions in Fig. 1h correspond to the $\sqrt{3}$ silicide islands. Magnified images of the darker region have disordered structure as in the case of 1 ML (see Fig. 1g and i), and are most possibly attributed to the bare Si surface. The shape of the $\sqrt{3}$ silicide islands is not as roundish as the case with 1 ML, but are rather meandering, or speckled. This meandering feature is probably a trace of coalescence of the $\sqrt{3}$ silicide islands as they grow in the lateral direction.

The effects of heating at higher temperatures, heating at 900 K for 15 s, are shown in Fig. 2a–c for 1 ML and Fig. 2d for 2 ML. In contrast to the case with heating at 800 K, the (7×7) spots in the RHEED pattern (Fig. 2a) are sharper and stronger indicating a good ordering in the (7×7) structure. The $\sqrt{3}\times\sqrt{3}$ streaks appear sharper which also shows an enhanced long-range order on the $\sqrt{3}$ silicide islands compared with the case with heating at 800 K. This is clearly understood from the corresponding STM pictures (Fig. 2b and c). The bare Si(111)-(7×7) regions show a good long-range order (inset in Fig. 2b). This implies that the destroyed (7×7) structure due to the reaction with Mn is recovered at this temperature. There are no irregular Mn clusters and only the $\sqrt{3}$ silicide islands are visible. The average size of the $\sqrt{3}$ silicide islands is larger than that in the case of heating at 800 K; some of them range up to 500 Å. Also, the height of the $\sqrt{3}$ silicide islands become higher (mostly 8 and 12 Å). Surface structure of the islands appears to be the same $\sqrt{3}$ structure irrespective of the island height. This point is different from the Er silicide on Si(111) which also forms tabular islands but different superstructures depending on the island height [5]. From the comparison of Fig. 2b and c, one can see the role of the steps in the silicide formation. In the case of high step density (Fig. 2b), the craters around the $\sqrt{3}$ silicide islands are absent since the Si atoms are sufficiently supplied from the step edges. In the case of low step density (Fig. 2c), supply of the Si atoms from the step edges is not sufficient. Thus, the Si atoms are

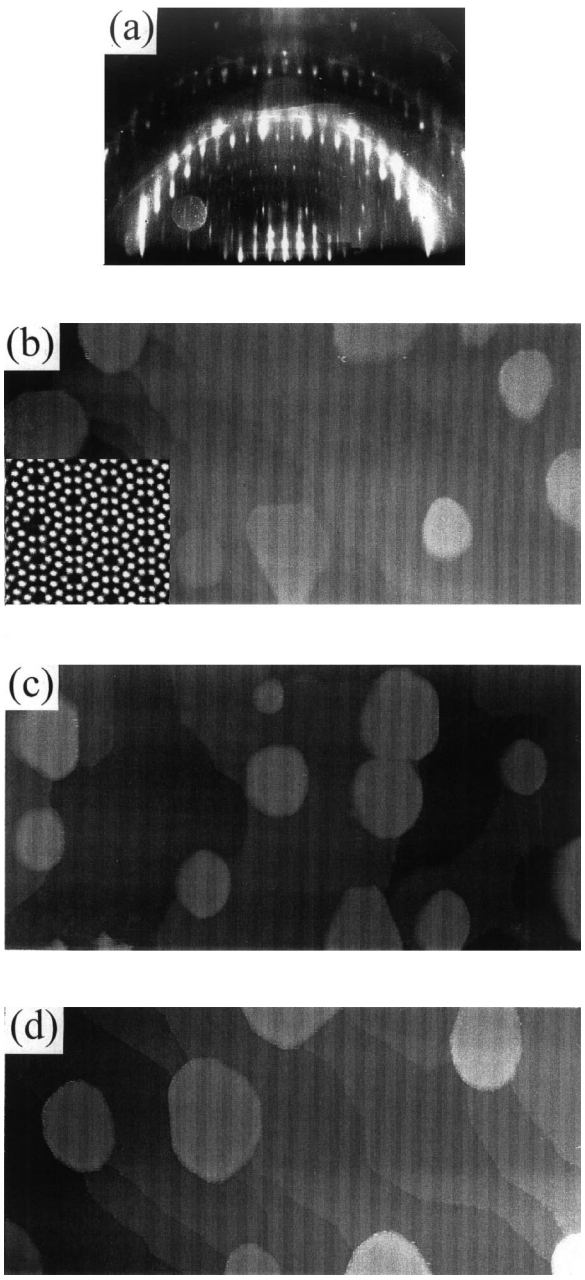

Fig. 2. (a) A RHEED pattern taken after depositing 1 ML of Mn at RT on the Si(111)-(7×7) surface and annealed at 900 K for 15 s. (b) Corresponding 3000 Å×1500 Å STM image taken at a region of high step density. (c) Corresponding 3000 Å×1500 Å STM image taken at a region of low step density. (d) A 3000 Å×1500 Å STM image of the surface heated at 900 K for 15 s after depositing 2 ML of Mn at RT. Inset in (b) shows a 54 Å×48 Å image of the (7×7) region in between the $\sqrt{3}$ silicide islands.

forcibly peeled off from the terraces and the subsequent silicide formation seems to proceed by taking the Si atoms from the step edges of the craters.

Fig. 2d corresponds to the surface heated at 900 K for 15 s with 2 ML of Mn. Compared with the 1 ML case (Fig. 2b and c), total area of the $\sqrt{3}$ silicide islands is almost the same (ca 20% of the total surface area), however, their height and size distributions shift toward higher values (e.g. 12 or 15 Å in height). Total volume of the $\sqrt{3}$ silicide islands does not increase completely in proportion as the deposited Mn amount; increase in the total volume of the $\sqrt{3}$ silicide islands is only 70% from Fig. 2b–d. Compared with the case of heating at 800 K, which only showed growth in lateral direction, silicide formation at 900 K shows stronger growth in vertical direction as well as in lateral direction. This results in the striking difference in the film morphology (see Figs. 1h and 2d).

A mechanism of the $\sqrt{3}$ silicide island formation is proposed as illustrated in Fig. 3 for the case of heating at 800 K. Mn atoms deposited at RT are weakly adsorbed on the surface and form small aggregates with keeping the morphology of the substrate (7×7) unit cell (Fig. 3a), corresponding to Fig. 1a and e. When the substrate is heated, the Mn clusters grow into one another (Fig. 3b), and some of the enlarged clusters start to react at defects such as small pits or step edges (Fig. 3c) to form $\sqrt{3}$ silicide islands. Evans et al. [4] suggested the possibility of size-dependent reactivity of the clusters as was observed in the Ag/Si(111) system [6]. For the present Mn/Si(111)-(7×7) system, Kawamoto et al. reported a transition from pure Mn phase to a metallic Mn–Si phase >5 ML [3]. The reported electronic state transition might be induced by the growth of Mn clusters by coalescing of small clusters with the increase of Mn coverage. In our case, though the coverage is <5 ML, increase in the cluster size (both in lateral and in perpendicular directions) is realized by the aggregation of the small Mn clusters by diffusion at elevated temperatures. After the reaction has started, the Mn clusters eat away the surface Si layer from step edges. When the stoichiometry of the cluster has reached to a certain value, the $\sqrt{3}$ silicide island will be formed

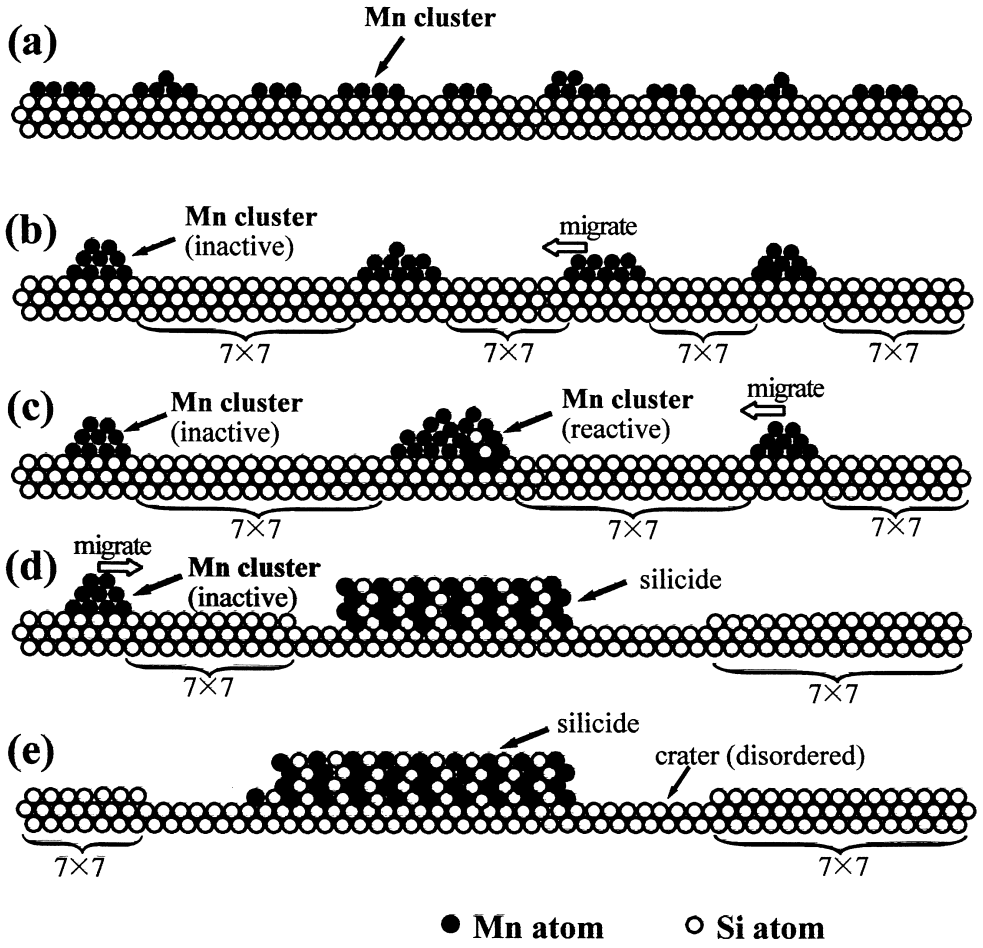

Fig. 3. Schematic illustrations for explaining the mechanism of Mn silicide formation on the Si(111)-(7×7) surface. ●, Mn atoms; ○, Si atoms.

(Fig. 3d). Other unreacted Mn clusters are subsequently merged into the $\sqrt{3}$ silicide islands to make the $\sqrt{3}$ silicide islands grow in the lateral direction (Fig. 3e). This merging of the unreacted Mn atoms will be achieved by the migration of the Mn cluster itself or by the indirect supply through the two-dimensional gas state formed by some of the Mn atoms possibly detached from the Mn clusters at elevated temperatures.

3.2. *Mn adsorbed on* $(\sqrt{3}\times\sqrt{3})$-*Ag,* α-$(\sqrt{3}\times\sqrt{3})$-*Au and* (6×6)-*Au*

Now we examine the reactivity and morphologies of Mn atomic layers grown on different surface structures formed by noble-metal pre-adsorption. Fig. 4a shows a $(\sqrt{3}\times\sqrt{3})$-Ag surface before Mn adsorption. Corrugation of this surface is small (0.2 Å) and the domain size is >300 Å. Fig. 4b shows the surface after depositing 1 ML of Mn and heated at 700 K for 15 s. In case of (7×7) when annealed at this temperature for the same period, most Mn atoms aggregates on terraces and very small amount of $\sqrt{3}$ silicide islands are seen mostly at steps. RHEED pattern corresponding to the surface of Fig. 4b is identical to that of the original surface except slightly increased background. Flat irregular clusters, most possibly identified as aggregates of unreacted Mn, are seen mostly at step edges. This shows the inertness of

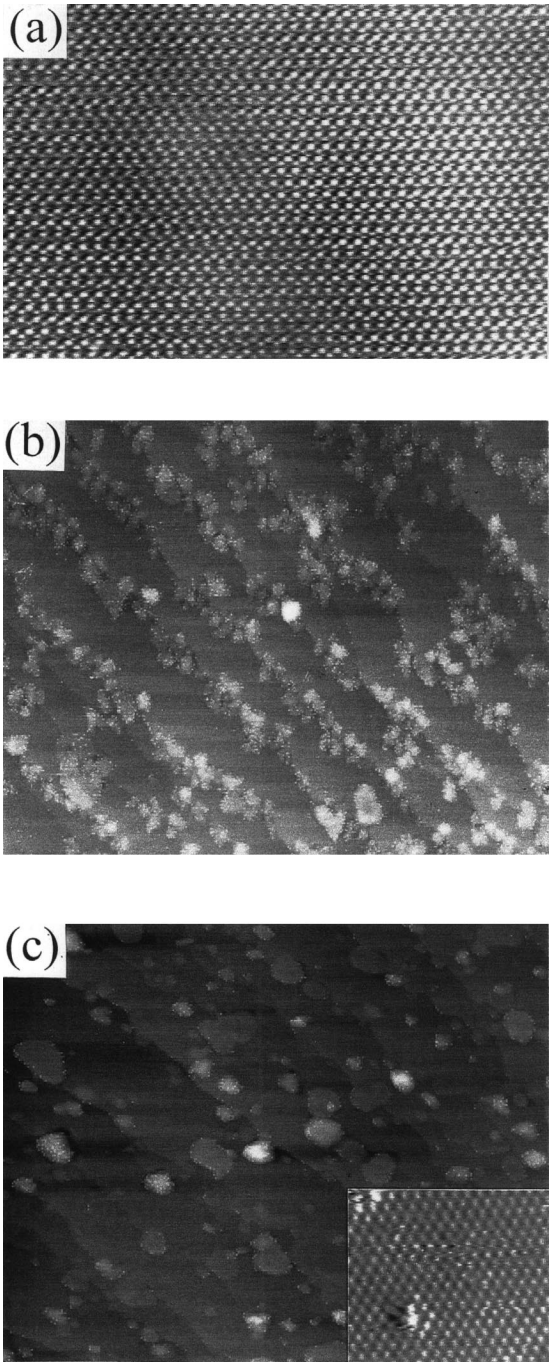

Fig. 4. (a) A 240 Å × 160 Å STM image of the $\sqrt{3}\times\sqrt{3}$-Ag surface. (b) A 6300 Å × 5100 Å image of the Mn adsorbed $\sqrt{3}\times\sqrt{3}$-Ag surface after heating at 700 K for 5 s. (c) A 6300 Å × 5100 Å image taken after successive heating at 700 K for 900 s of the surface (b). Inset shows 90 Å × 80 Å image on a $\sqrt{3}$ silicide island.

the $(\sqrt{3}\times\sqrt{3})$-Ag terraces and consequently the large diffusion length (>500 Å) of Mn atoms on them. Aggregation at the steps indicates high energy barriers for Mn atoms diffusing across the steps. In Fig. 4c, an effect of further heating is shown (700 K, 900 s). The RHEED pattern of this surface is identical to Fig. 1b except the absence of (7×7) spots. The flat $\sqrt{3}$ islands formed at step edges appear the same as those observed on Mn/Si(111)-(7×7) indicating that they are silicide. The remaining parts of the surface appear identical to that of the original $(\sqrt{3}\times\sqrt{3})$-Ag surface which has smaller corrugation than the $\sqrt{3}$ silicide islands' surface. Compared to the case with Mn/Si(111)-(7×7), formation of manganese silicide on the $(\sqrt{3}\times\sqrt{3})$-Ag surface is strongly restricted at step edges. This indicates that the $(\sqrt{3}\times\sqrt{3})$-Ag structure on terraces are rather stable and Si atoms are selectively stripped off from the steps where the $(\sqrt{3}\times\sqrt{3})$-Ag structure is less stable. However, the starting temperatures for the $\sqrt{3}$ silicide formation for both surfaces are almost the same.

STM images of Mn/α-$(\sqrt{3}\times\sqrt{3})$-Au and Mn/(6×6)-Au surfaces are shown in Fig. 5. Fig. 5a shows the α-$(\sqrt{3}\times\sqrt{3})$-Au surface before Mn adsorption. In contrast to the $(\sqrt{3}\times\sqrt{3})$-Ag surface, this surface is heavily corrugated due to the high density domain walls [7,8]. The electronic state variation as can be seen in STM topographic images will, in some way, result in the potential variation felt by adatoms. Thus, the domain walls as shown in Fig. 5a are expected to accompany potential walls (or moats) which hinders the diffusion of the adsorbed atoms. In fact, in contrast to Fig. 4b, drifts of adsorbed Mn atoms are not observed even after heating at 800 K, which indicates that the diffusion of Mn atoms on this surface is severely hindered (Fig. 5b); Mn clusters uniformly distribute on the surface irrespective of the step edge distributions. Above 800 K, reaction of Mn occurs. Again, distribution of the $\sqrt{3}$ silicide islands is rather uniform compared to the case with (7×7) and $(\sqrt{3}\times\sqrt{3})$-Ag. Around the flat $\sqrt{3}$ silicide islands, craters of 3 Å deep accompany. Since the structure at the bottom of the craters is also α-$(\sqrt{3}\times\sqrt{3})$-Au like on terraces, it is strongly

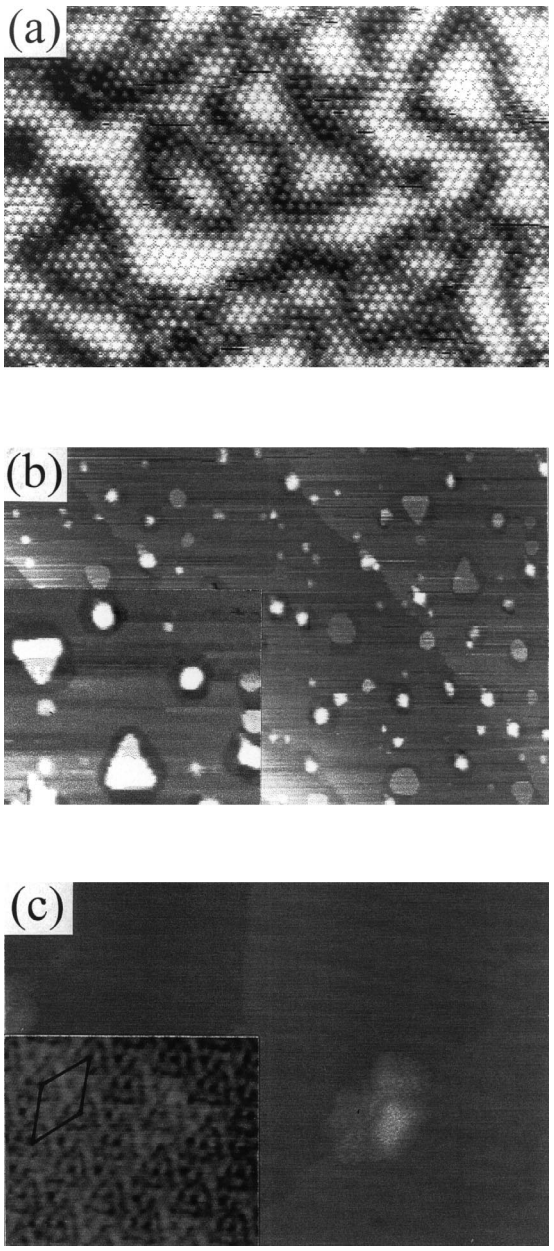

Fig. 5. (a) A 300 Å × 200 Å STM image of the $(\sqrt{3}\times\sqrt{3})$-Au surface. (b) A 6300 Å × 4200 Å image of the Mn adsorbed $(\sqrt{3}\times\sqrt{3})$-Au surface after heating at 800 K for 15 s. Inset shows a 1500 Å × 1200 Å image of the same surface. (c) A 2500 Å × 1700 Å image of the Mn adsorbed (6×6)-Au surface after heating at 870 K for 15 s. Inset shows a 115 Å × 90 Å image of (6×6)-Au structure. Note that if the surface is quench cooled, the $\beta-(\sqrt{3}\times\sqrt{3})$ surface is formed instead of the (6×6) surface, similar to the (6×6)-Au surface without Mn adsorption. For details, see Refs [7,8].

suggested that the Au atoms are not incorporated into the $\sqrt{3}$ silicide islands, and they are left on the craters to form again the α-$(\sqrt{3}\times\sqrt{3})$-Au overlayer after Si layers are removed to be incorporated into the $\sqrt{3}$ silicide islands. Starting temperature for the silicide formation is 100 K higher than on the (7×7) or the $(\sqrt{3}\times\sqrt{3})$-Ag surface. This is explained by the high stability of the α-$(\sqrt{3}\times\sqrt{3})$-Au terrace itself against Mn, and by the strong suppression of Mn diffusion by the domain walls which hinders Mn atoms from reaching the step edges where the α-$(\sqrt{3}\times\sqrt{3})$-Au structure is expected to be less stable and Si supply is easier. It is known that the α-$(\sqrt{3}\times\sqrt{3})$-Au surface undergoes melting of domain walls at 800 K [7]. Thus, the starting of the silicide formation at 800 K seems to have strong correlation with this domain-wall-melting.

Different from any cases shown above, the (6×6)-Au surface showed no formation of the $\sqrt{3}$ silicide islands as shown in Fig. 5c. RHEED pattern of this surface shows sharp (6×6) spots with weak complex transmission pattern. Almost all the surface area shows the same (6×6) structure as the original surface (see inset of Fig. 5c) and huge irregular clusters (possibly Mn clusters) are sparsely scattered over the surface. At higher temperatures above 1000 K, these clusters evaporate from the surface. These behaviors can be explained in terms of the large diffusion length of Mn atoms on the surface due to the small corrugation and the inertness of the (6×6)-Au surface.

4. Summary

Growth and morphology of quasi-two-dimensional Mn silicide on clean and noble-metal-precovered Si(111) surfaces have been studied by STM and RHEED. Heating at 800 K, adsorbed Mn atoms on Si(111)-(7×7) aggregate and react with the substrate at defects (in most cases at step edges) to form Mn silicide islands terminated with a $(\sqrt{3}\times\sqrt{3})$ superstructure. At this temperature, growth of this $\sqrt{3}$ silicide islands proceeds mostly in lateral direction with Mn coverage. At 900 K, growth in the vertical direction as well as in the

lateral direction become more significant than at 800 K. Morphology change of the Mn/Si(111)-(7×7) system is summarized in Fig. 6. The $(\sqrt{3}\times\sqrt{3})$-Ag surface is very stable against Mn adsorption at 700 K, and consequently Mn atoms diffuse largely and react selectively at step edges to form the $\sqrt{3}$ silicide islands. On the contrary, diffusion of Mn atoms on the α-$(\sqrt{3}\times\sqrt{3})$-Au

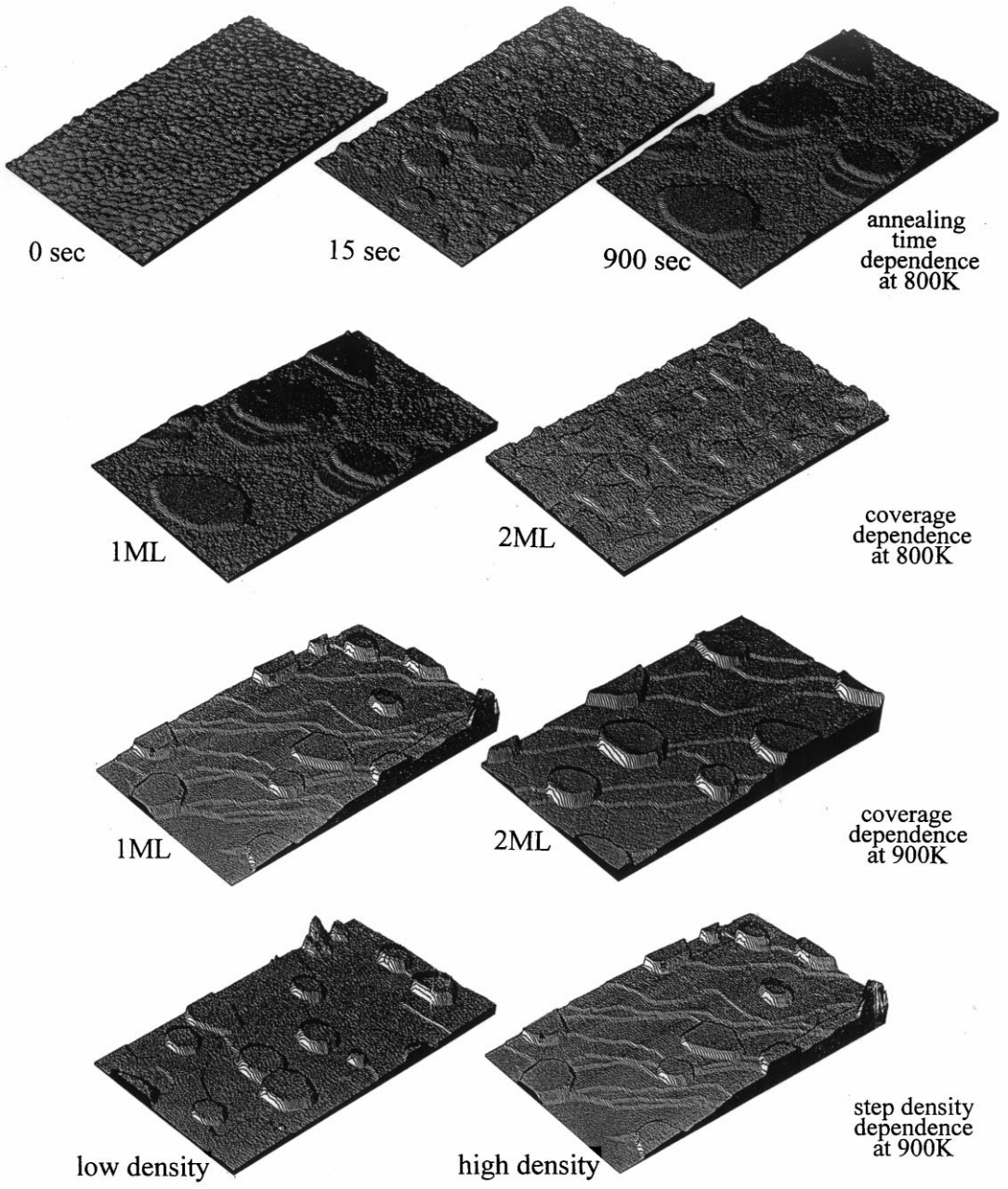

Fig. 6. A bird's-eye view of the Mn/Si(111)-(7×7) surfaces prepared by different annealing time, different annealing temperature, different Mn coverage, and with different step density.

surface is suppressed most possibly due to heavy surface corrugation accompanying the high-density domain walls, and no preferential reaction sites such as step edges are recognized. Mn atoms on the (6×6)-Au surface were found to aggregate easily and form no silicide possibly due to the small corrugation and the inertness of the surface.

Acknowledgements

This work has been supported in part by Grants-in-Aid from the Ministry of Education, Science, Culture, and Sports of Japan, especially through the Grant-in-Aid for Creative Basic Scientific Research (No. 08NP1201) conducted by Professor K. Yagi of Tokyo institute of Technology. One of the authors (T.N.) is supported by the Japan Securities Scholarship Foundation and Nippon Sheet Glass Foundation for Materials Science and Engineering.

References

[1] I. Kawasumi, M. Sakata, I. Nishida, K. Masumoto, J. Mater. Sci. 16 (1981) 355.
[2] Y.C. Lian, L.J. Chen, Appl. Phys. Lett. 48 (5) (1986) 359.
[3] S. Kawamoto, M. Kusaka, M. Hirai, M. Iwami, Surf. Sci. 242 (1991) 331.
[4] M.M.R. Evans, J.C. Glueckstein, J. Nogami, Phys. Rev. B 53 (1996) 4000.
[5] P. Wetzel, S. Saintenoy, C. Pirri, D. Bolmont, G. Gewinner, T.P. Roge, F. Palmino, C. Savall, J.C. Labrune, Surf. Sci. 355 (1996) 13.
[6] A. Shibata, Y. Kimura, K. Takayanagi, Surf. Sci. 303 (1994) 161.
[7] T. Nagao, S. Hasegawa, K. Tsuchie, S. Ino, C. Voges, H. Pfnuer, G. Klos, M. Henzler, Phys. Rev. B 57 (1998) 10100.
[8] T. Nagao, C. Voges, H. Pfnuer, M. Henzler, S. Ino, S. Hasegawa, Appl. Surf. Sci. 130–132 (1998) 47–53.